

# Cosmological constraints on Lorentz violating dark energy

B. Audren<sup>a</sup>, D. Blas<sup>b</sup>, J. Lesgourgues<sup>a,b,c</sup>, S. Sibiryakov<sup>d,e</sup>

<sup>a</sup> *FSB/ITP/LPPC, École Polytechnique Fédérale de Lausanne,  
CH-1015, Lausanne, Switzerland*

<sup>b</sup> *Theory Group, Physics Department, CERN, CH-1211 Geneva 23, Switzerland*

<sup>c</sup> *LAPTh (CNRS - Université de Savoie), BP 110, F-74941 Annecy-le-Vieux Cedex, France*

<sup>d</sup> *Institute for Nuclear Research of the Russian Academy of Sciences,  
60th October Anniversary Prospect, 7a, 117312 Moscow, Russia and*

<sup>e</sup> *Faculty of Physics, Moscow State University, Vorobjevy Gory, 119991 Moscow, Russia*

The role of Lorentz invariance as a fundamental symmetry of nature has been lately reconsidered in different approaches to quantum gravity. It is thus natural to study whether other puzzles of physics may be solved within these proposals. This may be the case for the cosmological constant problem. Indeed, it has been shown that breaking Lorentz invariance provides Lagrangians that can drive the current acceleration of the universe without experiencing large corrections from ultraviolet physics. In this work, we focus on the simplest model of this type, called  $\Theta$ CDM, and study its cosmological implications in detail. At the background level, this model cannot be distinguished from  $\Lambda$ CDM. The differences appear at the level of perturbations. We show that in  $\Theta$ CDM, the spectrum of CMB anisotropies and matter fluctuations may be affected by a rescaling of the gravitational constant in the Poisson equation, by the presence of extra contributions to the anisotropic stress, and finally by the existence of extra clustering degrees of freedom. To explore these modifications accurately, we modify the Boltzmann code CLASS. We then use the parameter inference code MONTE PYTHON to confront  $\Theta$ CDM with data from WMAP-7, SPT and WiggleZ. We obtain strong bounds on the parameters accounting for deviations from  $\Lambda$ CDM. In particular, we find that the discrepancy between the gravitational constants appearing in the Poisson and Friedmann equations is constrained at the level 1.8%.

## I. INTRODUCTION

Explaining the origin of the current acceleration of the universe is one of the biggest challenges in cosmology. Despite the great successes of the  $\Lambda$ CDM paradigm, it is hard to accept that a very fine-tuned form of otherwise invisible energy governs nowadays the behavior of the universe at the largest scales. A whole plethora of models are proposed as alternatives to this situation. These are known as *quintessence* or *dark energy* models [1–3]. The motivations and domain of applicability of various proposals are quite diverse: whereas some of them are intended as mere phenomenological models only valid for cosmology, others are rooted in theoretical considerations and are testable by different types of experiments. From the theoretical viewpoint the preferred models are those addressing (at least partially) the naturalness problem of the cosmological constant without introducing any additional fine-tunings. In this paper we will study in detail the  $\Theta$ CDM proposal of Ref. [4] that has such a property. This model is well-motivated theoretically and has a rich phenomenology that may distinguish it from  $\Lambda$ CDM.

The  $\Theta$ CDM model is based on the idea that the Lorentz invariance observed in the Standard Model of particle physics is an emergent phenomenon and does not correspond to a symmetry of nature. This concept is motivated by attempts to find complete theories of quantum gravity, but it can also be considered independently. There exist two different approaches: on one

hand Einstein-aether theory [5, 6] provides a phenomenological description of gravity with broken Lorentz symmetry at large distances; on the other hand Hořava gravity [7, 8] invokes a violation of Lorentz invariance at any scale to improve the quantum properties of gravitational theories. The restriction of Hořava gravity to operators with the lowest dimension can be considered as an effective theory by itself, called the *khronometric* theory [9]. The two proposals are very similar at large distances: the khronometric theory can be viewed as a constrained version of the Einstein-aether theory, and in many situations the predictions of the two theories coincide [9, 10]. The analysis presented in this work is applicable to all these classes of models. However, in the last step consisting in deriving the actual observational bounds on the model parameters, we will restrict to the khronometric case.

Several implications of the above models for cosmology have been studied in the past, see e.g. [11–17]. For the evolution of the Universe as a whole, the consequences of the minimal models<sup>1</sup> are rather trivial. They are compatible with Friedmann–Robertson–Walker (FRW) solutions that differ from the standard case only by a renormalization of the gravitational constant away from the value

<sup>1</sup> By this term we refer to the models with a minimal number of additional degrees of freedom in the gravity sector, and the simplest kinetic action (Einstein-aether and khronometric theories) [6, 9].

measured in local tests of Newton’s law. In other words, those models do not modify the form of the Friedmann equation. The background evolution becomes more interesting when non-minimal models are considered. In this case, the breaking of Lorentz invariance allows for Lagrangians which can change the expansion history of the universe and provide new alternatives for inflationary dynamics, dark matter and dark energy [4, 11, 17, 18]. Some criteria are necessary to identify the most interesting cases. In this work we will be concerned with the issue of dark energy, for which one would like to find a simple model described by a Lagrangian with high cutoff scale, that provides a mechanism to accelerate the universe insensitive to UV corrections<sup>2</sup> and distinguishable from  $\Lambda$ CDM. The  $\Theta$ CDM model of Ref. [4] meets these requirements.

Some consequences of  $\Theta$ CDM have been already discussed in Ref. [4]. In the present work we describe the observable physical effects of the model on cosmic microwave background (CMB) anisotropies and on the matter power spectrum (at the linear level). We provide a detailed discussion of such effects, that we computed accurately with a modified version of the flexible Boltzmann code CLASS [19]. We then compare the  $\Theta$ CDM model to recent CMB and Large Scale Structure (LSS) data using the Monte Carlo parameter inference code MONTE PYTHON [20].

Our work is organized as follows: in Sec. II we describe the  $\Theta$ CDM model and discuss the constraints not related to cosmology. In Sec. III we study the background evolution and derive linear equations for perturbations around the FRW background. The results presented in this section are complementary to those in Ref. [4]. They hold in a different gauge, and refer to different conventions and parametrizations, found to be more suitable for the numerical implementation. The qualitative effects of  $\Theta$ CDM on the CMB and matter power spectrum are described in Sec. IV. We present constraints from CMB and LSS data in Sec. V, and expose our conclusions in Sec. VI. Appendix A contains the derivation of initial conditions for cosmological perturbations in  $\Theta$ CDM.

## II. LORENTZ BREAKING THEORIES OF GRAVITY AND $\Theta$ CDM

Lorentz invariance is one of the best tested symmetries of the Standard model of particle physics [21]. It is also a fundamental ingredient of the theory of general relativity, that provides a very successful description of gravitational interactions over a huge range of scales. However, it is not known how to directly promote general relativ-

ity to a complete quantum theory, which points towards the necessity to consider alternatives. Independently of this, modifications to general relativity are currently being considered in the area of cosmology. The rationale behind these modifications is the possibility to use the wealth of cosmological data to learn how gravitation behaves at the largest accessible distances and, hopefully, shed some light on the mechanism responsible for the accelerated expansion of the universe.

These two lines of research converge if one assumes that Lorentz invariance is not a symmetry of the gravitational sector. This idea opens the possibility to construct gravitational theories with better quantum behavior than general relativity [7]. This is achieved at the price of introducing new degrees of freedom that modify the laws of gravity at all distances, including those relevant for cosmology [8, 9]. Even before this top-down approach had been initiated, the bottom-up Einstein-aether model [5] was proposed as a way to capture the large-distance effects of a putative Lorentz violation due to quantum gravity. In this work, we will consider theories where Lorentz violation is described by a preferred time-like vector field  $u_\mu$  defined at every point of space-time, which includes Einstein-aether theory and Hořava gravity. For the latter, we will focus only on its low-energy form, the khronometric theory [9]. The vector field will be normalized to<sup>3</sup>

$$u_\mu u^\mu = -1. \quad (1)$$

The presence of this dynamical field allows to use for the description of Lorentz violation the same language as for spontaneous symmetry breaking. Gravitational physics at large distances is governed by the following covariant action for  $g_{\mu\nu}$  and  $u_\mu$ , featuring a minimal number of derivatives:

$$S_{[\text{EH}u]} = \frac{M_0^2}{2} \int d^4x \sqrt{-g} [R - K^{\mu\nu}{}_{\sigma\rho} \nabla_\mu u^\sigma \nabla_\nu u^\rho + l(u_\mu u^\mu + 1)], \quad (2)$$

where

$$K^{\mu\nu}{}_{\sigma\rho} \equiv c_1 g^{\mu\nu} g_{\sigma\rho} + c_2 \delta_\sigma^\mu \delta_\rho^\nu + c_3 \delta_\rho^\mu \delta_\sigma^\nu - c_4 u^\mu u^\nu g_{\sigma\rho}, \quad (3)$$

and  $l$  is a Lagrange multiplier that enforces the unit-norm constraint. Equation (2) includes the Einstein-Hilbert (EH) term evaluated with the metric  $g_{\mu\nu}$ . The parameter  $M_0$  is proportional to the Planck mass (cf. (8)) while the dimensionless constants  $c_a$ ,  $a = 1, 2, 3, 4$ , characterize the strength of the interaction of the aether  $u_\mu$  with gravity. This is the action of the Einstein-aether model [5, 6].

<sup>2</sup> We leave aside the “old cosmological constant problem”: to find a mechanism imposing a null vacuum energy (see however the related comments in [4].)

<sup>3</sup> We use the  $(-+++)$  signature for the metric. This differs from most of the previous works in the field, but is common in cosmology.

The khronometric case corresponds to the situation where  $u_\mu$  is defined as a vector normal to a foliation consisting of the level surfaces of the *khronon* field  $\varphi$ ,

$$u_\mu \equiv \frac{\partial_\mu \varphi}{\sqrt{-\nabla^\nu \varphi \partial_\nu \varphi}}. \quad (4)$$

In this case, the constraint (1) is satisfied identically and the first term of (3) can be expressed as a linear combination of the last two terms. Thus,  $K^{\mu\nu}{}_{\sigma\rho}$  reduces to its last three terms with coefficients

$$\lambda \equiv c_2, \quad \beta \equiv c_3 + c_1, \quad \alpha \equiv c_4 + c_1. \quad (5)$$

At the level of linear perturbations, the khronometric theory differs from the Einstein-aether theory by the number of propagating degrees of freedom apart from the spin-two mode of the graviton. While the aether in general describes vector and scalar excitations, the khronometric case only contains scalars. However, the scalar sectors of the two theories are equivalent and are completely characterized by the three parameters (5).

Once the couplings to matter are specified, the constants  $c_a$  are constrained by various considerations ranging from theoretical requirements to observational tests. First, to very good precision, the Standard Model fields must couple only to  $g_{\mu\nu}$  and not to  $u_\mu$ , as required by Lorentz invariance in this sector<sup>4</sup> [21]. This decoupling presents a serious challenge to the proposal, but it is conceivable to achieve it either by imposing extra symmetries, e.g. supersymmetry [23, 24], or through a renormalization group running [25]. Next, there are restrictions imposed by the stability of Minkowski spacetime [6]. In particular, the requirement that the scalar mode is neither a ghost nor a tachyon field amounts to the constraints

$$0 < \alpha < 2, \quad \beta + \lambda > 0. \quad (6)$$

Stringent bounds come from observations of the Solar System dynamics, which can be used to place constraints on post-Newtonian (PPN) parameters. Two of these parameters, denoted by  $\alpha_1^{PPN}$  and  $\alpha_2^{PPN}$ , describe the effects of Lorentz violation. In general, they are different from zero (their value in general relativity) both in the Einstein-aether and khronometric theory; we refer the reader to [6, 29] for explicit relations with the constants  $c_a$ . Assuming no cancellations in these formulae, one obtains experimental bounds of the order of

$$|c_a| \lesssim 10^{-7}. \quad (7)$$

However, there are regions in the space of model parameters  $(\alpha, \beta, \lambda)$  in which  $\alpha_{1,2}^{PPN}$  vanish and Solar System

tests are automatically satisfied, with Newton's constant given by

$$G_N \equiv \frac{1}{8\pi M_0^2(1 - \alpha/2)}. \quad (8)$$

This requires<sup>5</sup>

$$\alpha = 2\beta \quad \text{for the khronometric model,} \quad (9a)$$

$$\alpha = -(3\lambda + \beta) \quad \text{for the Einstein-aether.} \quad (9b)$$

In these cases, much weaker bounds can be inferred from gravitational wave emission in binary systems [28, 29], giving

$$|c_a| \lesssim 10^{-2}, \quad (10)$$

and from the form of black hole solutions, imposing inequalities detailed in [26]. We will see that in the case of the khronometric model, the bounds that can be inferred from cosmology are competitive with (10), but not with (7). Thus we will impose the relation (9a) when searching for the allowed parameter space. Previous studies of the cosmological effects of Lorentz violation [11, 16] focused on the Einstein-aether model. In those works, the relation (9b) was enforced to avoid the PPN constraints. As we will explain, the relation (9b) also incidentally suppresses the leading effects in cosmology, unlike the relation (9a). This explains why the bounds obtained in those studies are rather mild.

The implications of the action (2) for the background evolution of an homogeneous and isotropic universe are minimal. If all matter components are universally coupled<sup>6</sup> to  $g_{\mu\nu}$ , the only difference with respect to general relativity is that the Friedmann equation involves a renormalized gravitational constant

$$G_{cos} \equiv \frac{1}{8\pi M_0^2(1 + \beta/2 + 3\lambda/2)} \quad (11)$$

differing from the value  $G_N$  measured e.g. on earth or in the Solar System<sup>7</sup>, given by Eq. (8). In order to modify the expansion history of the universe, and find a candidate for dark energy, we need to add a new ingredient to the model. We want to do it in a way that preserves the

<sup>5</sup> The difference between the models is due to the contributions to  $\alpha_{1,2}^{PPN}$  from the vector polarizations that are present only in the Einstein-aether case.

<sup>6</sup> A priori, there is no reason why this must be true for the dark matter. Still, as shown in [27], even allowing for non-universal interactions between the dark matter and the aether does not change the background evolution. As our main focus in this paper is dark energy, we will assume that the dark matter has standard properties (namely, that it is a pressureless fluid, described at the fundamental level by a Lorentz invariant Lagrangian, and with universal coupling to  $g_{\mu\nu}$ ).

<sup>7</sup> The analysis of Big Bang Nucleosynthesis [14] sets a bound on the relative difference between the two,  $|G_{cos}/G_N - 1| \leq 0.13$ .

<sup>4</sup> More generally, a universal coupling of Standard Model fields to a fixed combination of  $g_{\mu\nu}$  and  $u_\mu$  is allowed. This reduces to the previous case by a redefinition of the metric [22].

simplicity of the proposal and its validity as a low-energy effective field theory. This is achieved by supplementing the action (2) with a new field  $\Theta$  invariant under the shift symmetry,

$$\Theta \mapsto \Theta + \text{const.} \quad (12)$$

The low-energy action for this field is<sup>8</sup>

$$S_{[\Theta]} = \int d^4x \sqrt{-g} \left( -\frac{g^{\mu\nu} \partial_\mu \Theta \partial_\nu \Theta}{2} + \kappa \frac{(u^\mu \partial_\mu \Theta)^2}{2} - \mu^2 u^\mu \partial_\mu \Theta \right), \quad (13)$$

and involves two free parameters  $(\kappa, \mu)$ . We will refer to the model resulting from the combination of the actions (13) and (2) (with a universal coupling between matter fields and  $g_{\mu\nu}$ ) as  $\Theta$ CDM [4]. The cosmological constant term is set to be exactly zero<sup>9</sup>. Two comments are in order. First, as an effective field theory,  $\Theta$ CDM provides a valid description of physics up to a cutoff scale of the order of  $\Lambda_c \sim \sqrt{c_a} M_P$ . The bounds (7) or (10) show that this cutoff scale may be only a few orders of magnitude below the Planck mass. Furthermore, in the khronometric case, the theory has a potential UV completion, since it is a sub-case of Hořava gravity [7]. Second, in the whole  $\Theta$ CDM action, only the last operator in (13) breaks the discrete symmetry  $\Theta \rightarrow -\Theta$ . This implies that from the viewpoint of the effective field theory, it is self-consistent to choose the coefficient in front of this operator to be much smaller than the UV cutoff. In spite of  $\mu$  being dimensionfull, the above symmetry guarantees that it is renormalized multiplicatively, and that no dangerous contributions proportional to  $\Lambda_c$  appear. In other words, the smallness of  $\mu$  is technically natural. This last observation is very important, since we are going to see that in the  $\Theta$ CDM model,  $\mu$  sets the scale of the current cosmic acceleration.

### III. COSMOLOGICAL SOLUTIONS OF $\Theta$ CDM

We are interested in describing the evolution of perturbations around homogeneous and isotropic solutions in the  $\Theta$ CDM model. We focus on scalar perturbations, and refer the reader to [13, 15, 30] for possible effects of vector and tensor modes. In the synchronous gauge, the

perturbed FLRW metric has the form,

$$g_{00} = -a(\tau)^2, \quad g_{0i} = 0, \\ g_{ij} = a(\tau)^2 \left[ \delta_{ij} + \frac{\partial_i \partial_j}{\Delta} h + 6 \left( \frac{\partial_i \partial_j}{\Delta} - \frac{1}{3} \delta_{ij} \right) \eta \right]. \quad (14)$$

Besides, for  $\Theta$  and the khronon (or the longitudinal component of  $u_\mu$  in the more general Einstein-aether case) we introduce

$$\Theta = \bar{\Theta}(\tau) + \xi, \quad \varphi = \tau + \chi. \quad (15)$$

The matter components are assumed to be cold dark matter (*cdm*), photons ( $\gamma$ ), neutrinos ( $\nu$ ) and baryons (*b*). We describe these components at the same level of approximation as in Ref. [31]. In particular, the dark matter is treated as a pressureless fluid universally coupled to the metric  $g_{\mu\nu}$ . We assume that it is comoving with the gauge, in order to eliminate the well-known residual freedom in the synchronous gauge. We now discuss how the gravitational equations are modified in  $\Theta$ CDM. These equations were derived in [4] using the conformal Newtonian gauge. Here we will rewrite the linearized equations in the synchronous gauge (14), and in a form optimized for numerical study with the Boltzmann code CLASS [19].

#### A. Background evolution

Deriving the equation of motion for  $\Theta$  from (13), one finds that the homogeneous part  $\bar{\Theta}(t)$  evolves as

$$\dot{\bar{\Theta}} = -\frac{\mu^2 a}{1 + \kappa} + \frac{C}{a^2}, \quad (16)$$

where  $C$  is an integration constant. Substituting this solution into the Friedmann equation (derived from the combination of the actions (2) and (13)) yields

$$H^2 = \frac{8\pi G_{cos}}{3} \left( \rho_\mu + \rho_s + \rho_d + \sum_{\text{other}} \rho_n \right), \quad (17)$$

where  $H \equiv \dot{a}/a^2$  and  $G_{cos}$  is given by (11). The first three contributions in the brackets come from the energy-momentum tensor of the  $\Theta$ -field and have the form,

$$\rho_\mu \equiv \frac{\mu^4}{2(1 + \kappa)}, \quad \rho_s \equiv \frac{C^2(1 + \kappa)}{2a^6}, \quad \rho_d = -\frac{\mu^2 C}{a^3}, \quad (18)$$

while  $\rho_n$ ,  $n = cdm, \gamma, \nu, b$ , stand for the densities of the standard matter components of the Universe.

Let us analyze Eq. (17). Recall that there is no cosmological constant at the fundamental level in the model. Instead, the first term in (17) plays the same role with an energy scale set<sup>10</sup> by  $\mu$ . As emphasized above,  $\mu$  does not

<sup>8</sup> A similar action with an additional potential term for  $\Theta$  breaking the shift symmetry (12) was considered in [18].

<sup>9</sup> One can entertain the possibility of finding a mechanism that would enforce the cancellation of the vacuum energy induced by quantum loops [4]. However, at present, we are not aware of any such mechanism. Thus, the vanishing of the cosmological constant should be taken merely as an assumption.

<sup>10</sup> Throughout the paper we assume that the combination  $1 + \kappa$  is of order one.

receive large radiative corrections, and thus this source of dark energy can naturally have an energy scale completely unrelated to the cutoff of the theory. The second term has the form of the contribution of stiff matter. Not to spoil Big Bang Nucleosynthesis (BBN),  $\rho_s$  must be smaller than about 30 times the density of radiation in the Universe at temperatures of the order of 10 MeV [32]. Thus, assuming that this contribution was already present at BBN<sup>11</sup>, due to its rapid decrease, it is completely negligible at later epochs. The third term in (17) behaves as the energy density of dust<sup>12</sup>, so one might be tempted to identify it with the dark matter. However, being the geometric mean of the first two, this term is always subdominant and cannot contribute a significant fraction of dark matter. Given these considerations, we will set  $C = 0$  henceforth.

## B. Cosmological perturbations

Let us introduce two time scales that appear in the analysis of the linear perturbations,

$$\tau_\alpha^{-1} \equiv \sqrt{\frac{8\pi G_{\text{cos}}}{\alpha}} \dot{\Theta}, \quad H_\alpha \equiv \frac{H_0}{\sqrt{\alpha}}, \quad (19)$$

where  $H_0 = 100 \text{ h km s}^{-1} \text{ Mpc}^{-1}$  is the current value of the Hubble constant today. It is also convenient to rescale the  $\Theta$ -fluctuation defining

$$\tilde{\xi} \equiv \frac{\sqrt{8\pi G_{\text{cos}}}}{H_0} \xi, \quad (20)$$

so that both fields ( $\chi, \tilde{\xi}$ ) have the dimension of time. The equations of motion for  $\chi$  and  $\tilde{\xi}$  read

$$\begin{aligned} \ddot{\chi} &= -2\mathcal{H}\dot{\chi} \\ &- \left[ k^2 c_\chi^2 + (1+B)\mathcal{H}^2 + (1-B)\dot{\mathcal{H}} + \frac{G_0}{G_{\text{cos}}\tau_\alpha^2} \right] \chi \\ &+ \frac{G_0}{G_{\text{cos}}} \frac{H_\alpha}{\tau_\alpha} \tilde{\xi} - \frac{c_\chi^2}{2} \dot{h} - 2\frac{\beta}{\alpha} \dot{\eta}, \end{aligned} \quad (21a)$$

$$\ddot{\tilde{\xi}} = -2\mathcal{H}\dot{\tilde{\xi}} - k^2 c_\Theta^2 \tilde{\xi} + \frac{k^2 c_\Theta^2}{H_\alpha \tau_\alpha} \chi, \quad (21b)$$

<sup>11</sup> We do not specify the origin of the field  $\Theta$  in this work. One possibility is to identify  $\Theta$  with the Goldstone boson of a spontaneously broken global symmetry. Then, the above assumption amounts to stating that the corresponding phase transition occurs before BBN. If it happens later, the picture may change, but it is hard to see how this option can be incorporated in a viable cosmological scenario.

<sup>12</sup> Note though, that its sign can be negative depending on the sign of  $C$ .

where we introduced the notations

$$\begin{aligned} G_0 &\equiv \frac{1}{8\pi M_0^2}, \quad \frac{G_{\text{cos}}}{G_0} \equiv \frac{1}{1 + \beta/2 + 3\lambda/2}, \\ B &\equiv \frac{\beta + 3\lambda}{\alpha}, \quad c_\chi^2 \equiv \frac{\beta + \lambda}{\alpha}, \quad c_\Theta^2 \equiv \frac{1}{1 + \kappa}, \end{aligned} \quad (22)$$

and

$$\mathcal{H} \equiv aH. \quad (23)$$

Note that the constants  $c_\chi, c_\Theta$  represent the sound speeds of the fields  $\chi$  and  $\xi$  at relatively short wavelengths, where these modes decouple from each other [4]. These two velocities are constant in time and we will treat them as quantities of order one, which is their natural order of magnitude from the point of view of effective field theory. Note that in general they can exceed one, so that the fields can be superluminal. In Lorentz violating theories, this does not lead to any causal paradoxes, see e.g. the discussion in Ref. [33].

We now present the linearized Einstein equations. There are four equations in the scalar sector corresponding to different components of the Einstein tensor  $G^\mu{}_\nu \equiv R^\mu{}_\nu - \frac{1}{2}\delta^\mu{}_\nu R$ . Only two of these equations are independent, but we write all of them for completeness. For the  $\delta G^0_0$  component we find

$$\left( k^2 \eta - \frac{1}{2} \frac{G_0}{G_{\text{cos}}} \mathcal{H} \dot{h} \right) = -4\pi a^2 G_0 \sum_n \rho_n \delta_n, \quad (24)$$

with

$$\begin{aligned} \sum_i \rho_i \delta_i &\equiv \sum_{\text{other}} \rho_i \delta_i + \frac{\alpha}{8\pi a^2 G_{\text{cos}} c_\Theta^2} \frac{H_\alpha}{\tau_\alpha} \dot{\tilde{\xi}} \\ &+ \frac{\alpha k^2}{8\pi a^2 G_0} (\mathcal{H}(1-B)\chi + \dot{\chi}). \end{aligned} \quad (25)$$

Here and in what follows, the label ‘other’ refers to contributions from the standard matter components, whose form can be found in [31]. For the  $\partial_i \delta G^0_i$  part we find

$$2k^2(1-\beta)\dot{\eta} - \frac{\alpha c_\chi^2}{2} k^2 \dot{h} = 8\pi a^2 G_0 \sum_n (\rho_n + p_n) \theta_n, \quad (26)$$

with

$$\sum_n (\rho_n + p_n) \theta_n \equiv \sum_{\text{other}} (\rho_n + p_n) \theta_n + \frac{\alpha c_\chi^2}{8\pi a^2 G_0} k^4 \chi. \quad (27)$$

The  $\delta G^i_i$  equation reads

$$\ddot{h} = -2\mathcal{H}\dot{h} + 2\frac{G_{\text{cos}}}{G_0} k^2 \eta - 24\pi G_{\text{cos}} a^2 \sum_i \delta p_n, \quad (28)$$

where

$$\sum_n \delta p_n \equiv \sum_{\text{other}} \delta p_n + \frac{\alpha B}{24\pi a^2 G_0} k^2 (\dot{\chi} + 2\mathcal{H}\chi). \quad (29)$$

Finally, the  $\partial_i \partial_j \delta G_j^i$  equation yields

$$(1 - \beta)(\ddot{h} + 6\ddot{\eta} + 2\mathcal{H}(\dot{h} + 6\dot{\eta})) - 2k^2\eta = -24\pi a^2 G_0 \sum_n (\rho_n + p_n)\sigma_n, \quad (30)$$

with

$$\sum_n (\rho_n + p_n)\sigma_n \equiv \sum_{\text{other}} (\rho_n + p_n)\sigma_n - \frac{\beta k^2}{12\pi a^2 G_0}(\dot{\chi} + 2\mathcal{H}\chi). \quad (31)$$

In the above expressions the pressure fluctuations  $\delta p_n$ , the velocity divergences  $\theta_n$  and the shear potentials  $\sigma_n$  are defined in the standard way, see [31]; the equations for perturbations in the matter components can be found in the same reference. The linearized equations must be supplemented by suitable initial conditions. The latter are derived in Appendix A.

For simplicity, we are going to set  $c_\Theta = 1$  in the numerical simulations. This prescription is equivalent to fixing  $\kappa = 0$ , and leaves us with four free fundamental parameters ( $\alpha, \beta, \lambda, \mu$ ). A different choice for  $c_\Theta$  would not affect qualitatively the evolution of perturbations, unless  $c_\Theta$  is very small. In that case, the field  $\xi$  could in principle cluster on scales much smaller than the Hubble radius, but we will not consider this situation in the present work<sup>13</sup>.

We can compare the number of free parameters in this model with that in an ordinary  $\Lambda$ CDM model sharing the same background evolution. The parameters ( $\Omega_\Lambda, H_0$ ) of  $\Lambda$ CDM can be mapped onto the parameters ( $\mu, H_0$ ) of the  $\Theta$ CDM model. Hence the latter features only three additional parameters ( $\alpha, \beta, \lambda$ ), reducing to only two independent parameters after imposing one of the conditions fulfilling Solar System tests, (9b) or (9a). Once ( $\alpha, \beta, \lambda$ ) are fixed, all coefficients in the field equations (21) and in the Einstein equations can be derived.

### C. Changing the gauge

Reference [31] shows the impact of a gauge transformation on the variables describing matter and metric perturbations, and on the form of their respective equations of evolution. Here we show how the fields  $\chi$  and  $\xi$  transform when switching from the synchronous to the Newtonian gauge. This transformation is induced by the particular change of coordinates

$$x^0 \mapsto x^0 - \dot{\beta}(x, \tau), \quad x^i \mapsto x^i - \partial_i \beta(x, \tau) - \epsilon^i(x), \quad (32)$$

where

$$\beta(x, \tau) = \int d^3k \frac{e^{ikx}}{2k^2} (h + 6\eta), \quad \partial_i \epsilon^i = 0. \quad (33)$$

After this transformation, the scalar part of the metric (14) becomes diagonal,

$$ds^2 = a(\tau)^2 [-(1 + 2\psi)d\tau^2 + (1 - 2\phi)dx^i dx_i], \quad (34)$$

with

$$\psi = \dot{\beta} + \mathcal{H}\beta, \quad \phi = \eta - \mathcal{H}\dot{\beta}. \quad (35)$$

The khronon and  $\Theta$  field transform as

$$\chi \mapsto \chi^N = \chi + \dot{\beta}, \quad \tilde{\xi} \mapsto \tilde{\xi}^N = \tilde{\xi} + \frac{\sqrt{8\pi G_{\text{cos}}}}{H_0} \dot{\Theta} \dot{\beta}. \quad (36)$$

Although the Boltzmann code CLASS features equations in both the synchronous and Newtonian gauge, for simplicity, we choose to implement the  $\Theta$ CDM equations in the synchronous gauge only. However, when presenting the physical interpretation of numerical results in the next section, we will refer to the evolution of quantities in the Newtonian gauge, obtained by performing the above transformation inside the code a posteriori (i.e. after solving the equations of motion in the synchronous gauge).

## IV. OBSERVABLE EFFECTS

The modified evolution of linear perturbations in  $\Theta$ CDM leads to observable consequences which we now discuss. We focus on the scalar sector, known to contribute most to observable quantities. The effects of Lorentz violation on the tensor and vector sectors are weakly constrained by current cosmological data [13, 15, 30]. The only effect on tensor modes is a small shift in their velocity [6]. The vector equations are identical in general relativity and in the khronometric model, implying that vector perturbations decay with time. Possible effects of vector modes in the Einstein-aether model on CMB polarization have been discussed in [13, 15].

At the qualitative level, one can identify three main effects distinguishing the growth of perturbations in  $\Theta$ CDM from that in  $\Lambda$ CDM. These are: (i) a rescaling of the matter contribution in the Poisson equation (i.e., a different self-gravity of matter perturbations), (ii) an additional contribution to the anisotropic stress, and (iii) the presence of additional clustering species. The first two effects are generic for any Lorentz violating gravitational theory based on the Einstein-aether or khronometric model<sup>14</sup>, while the third is specific to the dynamical realization of dark energy in  $\Theta$ CDM.

<sup>13</sup> A small value of  $c_\Theta$  corresponds to the near cancellation of the kinetic terms for  $\xi$  coming from the first and second terms in Eq. (13) - a situation that appears fine-tuned from the effective field theory perspective.

<sup>14</sup> Similar effects are also known in other modified gravity and dark energy models, see e.g. [34, 35].

To understand these effects, let us work in the Newtonian gauge. The Poisson equation (i.e., the sub-Hubble limit of the (00) Einstein equation) reads

$$k^2(2\phi - \alpha\psi) = -8\pi G_0 a^2 \sum_{\text{other}} \rho_n \delta_n - \alpha k^2 (\dot{\chi} + \mathcal{H}(1-B)\chi) - \frac{\alpha G_0}{c_{\Theta}^2 \tau_{\alpha} G_{\text{cos}}} \left( H_{\alpha} \dot{\xi} - \frac{\psi}{\tau_a} \right). \quad (37)$$

Let us first concentrate on the contribution of standard matter. Using the Friedmann equation (17), the (time-dependent) fraction of the total energy density of the Universe due to each matter component is given by

$$f_n \equiv \frac{8\pi G_{\text{cos}}}{3H^2} \rho_n. \quad (38)$$

The Poisson equation takes the form

$$\begin{aligned} k^2\phi &= -4\pi G_N a^2 \sum_{\text{other}} \rho_n \delta_n \\ &= -\frac{3}{2} \frac{G_N}{G_{\text{cos}}} \mathcal{H}^2 \sum_{\text{other}} f_n \delta_n, \end{aligned} \quad (39)$$

where for the time being we have omitted the terms in the second line of (37) and neglected the anisotropic stress (i.e. we have set  $\psi = \phi$ ). If we assume that the background evolution of the Universe is standard, with  $\mathcal{H}$  and  $f_n$  being exactly the same as in  $\Lambda$ CDM, Eq. (39) implies that the strength of the gravitational potential produced by density perturbations is modified by the factor  $G_N/G_{\text{cos}}$ . When this modified potential is substituted into the matter equations of motion (which have the standard form), it leads to a different growth rate of perturbations with respect to the  $\Lambda$ CDM case. For instance, a straightforward calculation shows that during the matter dominated epoch, the density contrast grows according to the modified power-law (cf. [12])

$$\delta \propto a^{\frac{1}{4}(-1 + \sqrt{1 + 24G_N/G_{\text{cos}}})}. \quad (40)$$

Notice that for small values of the parameters ( $\alpha$ ,  $\beta$ ,  $\lambda$ ) the anomalous growth is proportional to

$$\frac{G_N}{G_{\text{cos}}} - 1 = \frac{\Sigma}{2} + O(\alpha^2), \quad (41)$$

where we have defined

$$\Sigma \equiv \alpha + \beta + 3\lambda. \quad (42)$$

For  $\Sigma = 0$ , the effect of modified self-gravity is strongly suppressed. Hence we expect cosmological bounds on ( $\alpha$ ,  $\beta$ ,  $\lambda$ ) to be weaker along this degeneracy direction. Incidentally, in the Einstein-aether case  $\Sigma$  is required to vanish (or, rather, be extremely small) by the PPN constraints, see (9b). This explains why the cosmological bounds on Einstein-aether theory are rather mild [11, 16].

Model	$\alpha$	$\beta$	$\lambda$	$\Sigma$
<i>enhanced gravity</i>	0.2	0	0.1	0.5
<i>shear</i>	0.05	0.25	-0.1	0

TABLE I: Parameters for the *enhanced gravity* and *shear* models.

On the other hand, in the khronometric model the PPN constraints are compatible with  $\Sigma \neq 0$  and the influence of Lorentz violation on cosmological perturbations is more pronounced.

The second effect is understood from the tracefree part of the (*ij*) Einstein equation,

$$k^2(\psi - \phi) = -12\pi G_0 a^2 \sum_{\text{other}} (\rho_i + p_i)\sigma_i + \beta k^2(\dot{\chi} + 2\mathcal{H}\chi). \quad (43)$$

Since the khronon field introduces a preferred direction  $u_{\mu}$  in space-time, it may generate anisotropic stress. This effect (proportional to  $\beta$ ) is accounted for by the last term in the previous equation. Generally speaking, adding anisotropic stress amounts to increasing the viscosity of the cosmic fluid, and leads to a damping of small-scale perturbations.

The third effect comes from gravitational interactions between ordinary matter species and the scalar fields  $\chi$  and  $\xi$ . This interaction, described by the second line in Eq. (37), may play an important role under the condition that the fields cluster and form sufficiently dense clumps. This might be the case through a mechanism described in Ref. [4]. The mixing between the dark energy perturbation  $\xi$  and the khronon  $\chi$  (see Eqs. (21)) gives rise to a mode whose sound speed vanishes in the limit of small momentum  $k$ . This property implies that the effective pressure associated with the mode is small, and that the density perturbations ( $\delta\rho_{\chi}$ ,  $\delta\rho_{\xi}$ ) can be amplified efficiently by gravitational collapse. Hence, the  $\Theta$ CDM model features clustering dark energy. A semi-quantitative analysis of this effect was performed in [4], showing that structure formation is enhanced at small comoving momenta (large wavelengths),  $k \lesssim H_{\alpha}$ . Unfortunately, in this range, the quality of cosmological data is rather poor, and this effect does not play a significant role in actual observational constraints on the model.

To illustrate how the above effects impact observable quantities, we study numerically the evolution of cosmological perturbations in two reference models using the Boltzmann code CLASS. We will call them the *enhanced gravity* and the *shear* models. The corresponding parameter values are listed in Table I. Clearly, in the *enhanced gravity* model we keep the effect (*i*) while switching off the effect (*ii*); in the case of the *shear* model the situation is opposite. The effect (*iii*) is present in both models but we will see that it is always subdominant. Note that the values in Table I have been chosen very large in order

to make the modifications visible on the plots. However, these values are excluded by current data (see Sec. V).

### A. Effects on the CMB

In this subsection, we describe the changes induced by Lorentz violation in the CMB temperature anisotropy spectrum. We consider  $\Theta$ CDM with the two reference sets of parameters listed above and compare the results to  $\Lambda$ CDM. To highlight the changes, all simulations are performed with adjusted initial conditions such that, in the limit  $k \rightarrow 0$ , the gravitational potential  $\psi$  is the same for all three models. For the standard cosmological parameters, we choose the following values:  $n_s = 1$ ,  $h = 0.7$ ,  $\Omega_b = 0.05$ ,  $\Omega_{cdm} = 0.25$ ,  $A_s = 2.3 \times 10^{-9}$ ,  $z_{reio} = 10$ .

*Enhanced gravity model:* In Fig. 1 (top panel) we can see that at the time of decoupling, the gravitational potential in this model is enhanced (in absolute value) compared to  $\Lambda$ CDM. This is due to an increase in the perturbation growth, governed by  $\Sigma$ . On the same panel one observes two changes in the solution for the photon temperature perturbations  $\Theta_\gamma \equiv \delta_\gamma/4$ : a shift of the peaks of oscillations towards higher momenta, and a shift of the zero point of oscillations. These effects can be qualitatively understood from the combination of the modified Poisson equation (39) with the equations of motion of the photon-baryon plasma before decoupling. The latter have a standard form, and in the tight coupling approximation they reduce to a single master equation,

$$\ddot{\Theta}_\gamma + \frac{\dot{R}}{1+R} \dot{\Theta}_\gamma + k^2 c_s^2 \Theta_\gamma = -\frac{k^2}{3} \psi + \frac{\dot{R}}{1+R} \dot{\phi} + \ddot{\phi}, \quad (44)$$

where  $R \equiv \frac{3\rho_b}{4\rho_\gamma}$  encodes the baryon-to-photon density ratio, and  $c_s \equiv (3(1+R))^{-1/2}$  is the sound speed of density waves in the plasma in the absence of gravity. According to Eq. (39), the first term on the r.h.s. of (44) contains a contribution proportional to  $\Theta_\gamma$ . This contribution is positive and larger than in  $\Lambda$ CDM for  $\Sigma > 0$ . It effectively decreases the speed of sound in the plasma at the moment when each mode enters inside the horizon<sup>15</sup>, which translates into a shift of the peaks, observed in the top panel of Fig. 1. Next, the zero point of the acoustic oscillations is given by the value of  $-\psi/3c_s^2$  at decoupling. As already mentioned,  $|\psi|$  is larger in the *enhanced gravity* model, leading to a shift in this zero point further away from  $\Theta_\gamma = 0$ . Finally, the amplitude of the acoustic oscillations around the zero point is slightly smaller in the *enhanced gravity* model than in  $\Lambda$ CDM.

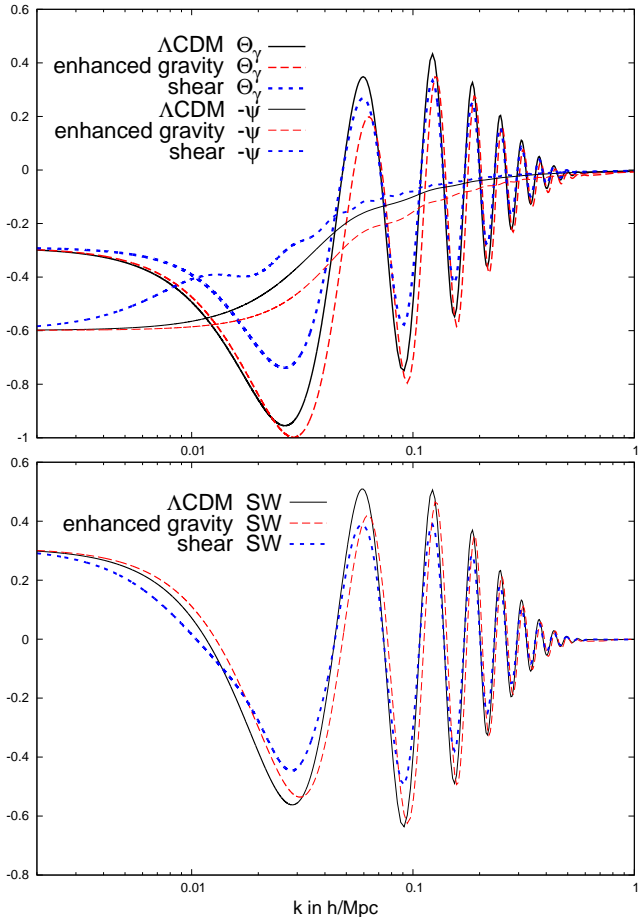


FIG. 1: Top: photon temperature perturbation  $\Theta_\gamma \equiv \delta_\gamma/4$  and gravitational potential  $-\psi$  at decoupling, for the three models under scrutiny. Bottom: Sachs-Wolfe contribution, given by  $\Theta_\gamma + \psi$  (i.e. by the difference between the two curves above).

The above features affect the Sachs-Wolfe (SW) contribution to temperature anisotropies. In the bottom panel of Fig. 1, we plot this contribution, given by  $\Theta_\gamma + \psi$  at recombination. One clearly sees the shift of the peaks and notices that the even peaks are suppressed while the odd ones are almost constant (with the notable exception of the first peak, which is suppressed). This is due to the competition between the different effects described in the previous paragraph.

In the anisotropies observed today, the SW contribution is supplemented by those coming from the Doppler and Integrated Sachs-Wolfe (ISW) effects. The decomposition of the  $C_\ell$  spectrum in terms of these effects is presented in Fig. 2 for different models. The comparison of the *enhanced gravity* model with  $\Lambda$ CDM is shown in the top-panel. In the SW contribution (as well as in the total spectrum), we observe the expected suppression of the first, second and fourth peaks, while the third peak amplitude is roughly unchanged. On small angular

<sup>15</sup> Strictly speaking, the Poisson equation (39) is valid only for sub-horizon modes. However, it is sufficient for our qualitative argument.



scales, the peaks are further suppressed by Silk damping. Indeed, due to the shift in the phase of oscillations, they correspond to smaller physical scales at recombination, that are more affected by diffusion damping. The Doppler effect, which depends on  $\dot{\Theta}_\gamma$  at recombination, is also modified. Finally, a prominent feature clearly visible on the plot is the significant enhancement of the ISW contribution in the range  $10 < l < 100$ , i.e. between the regions usually affected by the early ISW effect ( $100 < l < 200$ ) and the late ISW effect ( $2 < l < 10$ ). The ISW effect is proportional to the time derivative of the gravitational potential. In the  $\Lambda$ CDM model, the potential varies only during the epochs of radiation and  $\Lambda$  domination. However, in the *enhanced gravity* model, the growth of density perturbations entails a slow increase of the gravitational potential also during the matter dominated era, enhancing the ISW effect on a wide range of scales.

All in all, we conclude that the *enhanced gravity* model produces significant modifications in the spectrum of CMB anisotropies. The pattern of these modifications is quite specific, and apparently not degenerate with the effects of standard cosmological parameters.

*Shear model:* We recall that in this model, the  $\chi$  field generates some anisotropic stress and contributes to the shear of the perturbed metric, as described by Eq. (43). The presence of shear tends to smooth out metric perturbations on scales smaller than the sound horizon associated with the sound speed of the  $\chi$  field. Note that for parameters of the particular *shear* model studied here, the field  $\chi$  is superluminal<sup>16</sup> ( $c_\chi = \sqrt{3}$ ) and the suppression appears already on super-Hubble scales.

This is indeed observed on the top panel of Fig. 1, where the gravitational potential is clearly smaller (in absolute value) compared to  $\Lambda$ CDM. It also exhibits notable wiggles caused by oscillations in the  $\chi$ -field [4]. The fact that  $c_\chi$  is much larger than the photon-baryon sound speed explains the shift between the phase of the oscillations seen in  $\psi$  and in  $\Theta_\gamma$ . The suppression of  $\psi$  shifts the zero-point of the oscillations in the photon temperature  $\Theta_\gamma$ . On the other hand, we do not see any shift in the positions of the peaks, which is compatible with the previous discussion: the self-gravity of radiation is not modified in this model.

For fixed initial conditions  $\Theta_\gamma(\tau_0)$ , the amplitude of the acoustic oscillations depends crucially on boosting effects, imprinted around the time of Hubble crossing, and caused by the three gravitational driving terms on the right-hand side of Eq. (44). In the *shear* model, the amplitude of acoustic oscillations is damped as a consequence of smaller metric fluctuations and reduced gravitational boosting. This translates into an overall sup-

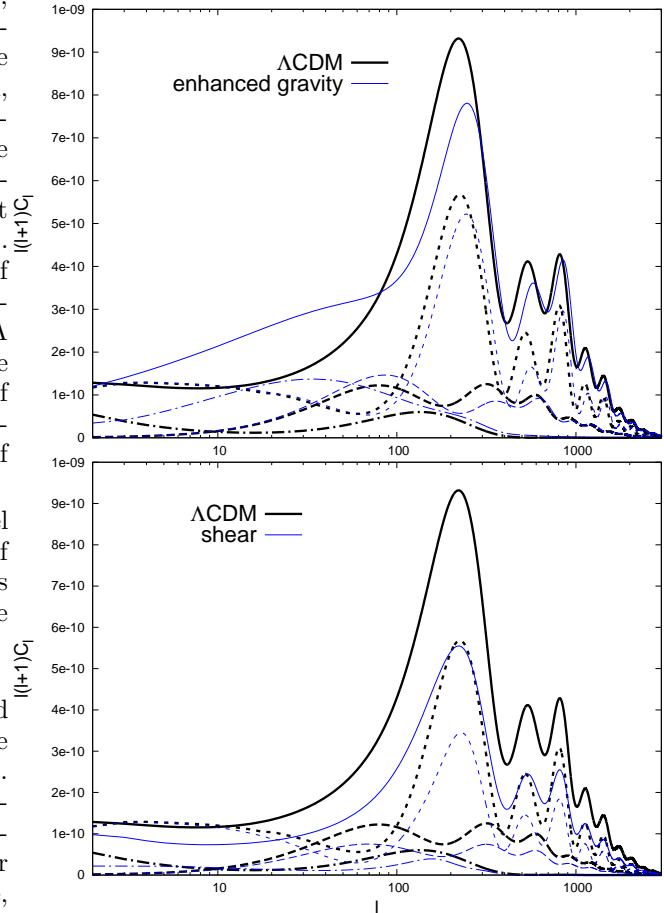


FIG. 2: Temperature anisotropy spectrum (solid) and its decomposition in terms of Sachs–Wolfe (dotted), Doppler (dashed) and Integrated Sachs–Wolfe (dot-dashed) contributions. For clarity, we do not show cross correlations between these contributions. Thick black lines represent the  $\Lambda$ CDM model, while thin blue lines are used for the two  $\Theta$ CDM reference models.

pression of the SW effect visible in the bottom panel of Fig. 1.

On Fig. 2, we see that the Doppler and ISW contributions to the total temperature spectrum  $C_\ell$  are also lower in the *shear* model than in  $\Lambda$ CDM. The net result is a uniform suppression of all peaks. One may expect that this effect could be compensated, at least partially, by a rescaling of the initial amplitude of perturbations. This suggests that pure *shear* models might be less constrained than *enhanced gravity* ones.

Our *shear* model is similar to the one studied in [11], where it was claimed that the dominant effect on the CMB comes through the ISW. Our analysis demonstrates that the changes in the SW and Doppler contributions are equally important for this model.

<sup>16</sup> As pointed above, this does not present any inconsistencies in theories without Lorentz invariance.

## B. Effects on the matter power spectrum

Another observable affected by the behaviour of cosmological perturbations in  $\Theta$ CDM is the matter power spectrum. We restrict the discussion to low enough Fourier modes,  $k \lesssim 0.1$  h/Mpc, for which perturbations are still very close to the linear regime. The study of non-linear clustering in this model is beyond the scope of the present paper.

The definition of what one calls the “matter power spectrum” is not so obvious in  $\Theta$ CDM. This model contains additional components that contribute to perturbations of the total energy density. One may wonder whether they must be included in the calculation of the power spectrum. In general, the answer to this question is yes. Indeed, the existing observations fall into two categories. The first category probes directly metric perturbations (themselves related to total density fluctuations): this is the case e.g. for cosmic shear surveys or CMB lensing measurements. The second category measures the clustering of compact objects like galaxies, halos or clusters. On large scales, these objects are known to trace linearly the underlying gravitational field [36]. Thus, it appears reasonable to *define* the matter power spectrum using the Poisson equation<sup>17</sup>

$$k^2\phi = -4\pi G_N a^2 \delta\rho_{tot}. \quad (45)$$

Note that we have used here the locally determined value of the Newton constant introduced in Eq. (8). Comparing Eq. (45) to Eq. (37) and neglecting the anisotropic stress which is very small on relevant scales, we see that the contribution of ordinary matter to  $\delta\rho_{tot}$  coincides with the standard definition  $\delta\rho_n$ , while the contributions of the khronon and  $\tilde{\xi}$  fields read

$$\begin{aligned} \delta\rho_\chi &\equiv \frac{\alpha k^2}{8\pi a^2 G_0} (\dot{\chi} + \mathcal{H}(1-B)\chi), \\ \delta\rho_\xi &\equiv \frac{\alpha}{8\pi a^2 G_{cos} c_\Theta^2 \tau_\alpha} \left( H_\alpha \dot{\tilde{\xi}} - \frac{\psi}{\tau_\alpha} \right). \end{aligned} \quad (46)$$

We stress that all quantities here are taken in the Newtonian gauge.

To obtain the matter power spectrum, the density perturbation  $\delta\rho_{tot}$  must be divided by the total matter density (dark matter plus baryons). The latter is determined from the background cosmological solution. In the case of standard gravity, one would again use the local Newton constant  $G_N$  to infer the density from the geometry. Because in the  $\Theta$ CDM model the gravitational constant in the Friedmann equation is different, the effective matter density found in this way is renormalized compared

to the actual value,

$$\rho_{\text{eff}} = \frac{G_{cos}}{G_N} (\rho_{cdm} + \rho_b). \quad (47)$$

Thus we arrive at the following formula for the power spectrum,

$$P(k) = \left( \frac{G_N}{G_{cos}} \right)^2 \frac{\langle |\delta\rho_{tot}(\vec{k})|^2 \rangle}{(\rho_{cdm} + \rho_b)^2}. \quad (48)$$

Let us discuss the imprint of our two reference  $\Theta$ CDM models on this spectrum.

*Enhanced gravity model:* The left panels of Fig. 3 show the time dependence of various contributions to  $\delta\rho_{tot}$  in this model, for three values of the momentum  $k$ . As expected, inside the Hubble radius, matter density perturbations grow at a larger rate and are enhanced compared to the  $\Lambda$ CDM case. The contribution of the  $\chi$  and  $\xi$  fields, though small, exhibits some interesting features. On super-Hubble scales, the  $\xi$ -density perturbation rapidly grows with time. This is due to the mixing between  $\chi$  and  $\tilde{\xi}$  discussed in Ref. [4], which gives rise to a mode with vanishing sound speed at low momenta, and allows for clustering of the dark energy. In the case of modes crossing the Hubble scale around the current epoch,  $\delta\rho_\xi$  even becomes comparable to the matter contributions at the present time. However, at shorter scales, the mixing between  $\chi$  and  $\tilde{\xi}$  disappears and the speeds of sound of these components become non negligible<sup>18</sup>. This leads to damped oscillations of these fields, clearly visible in the lower left panel of Fig. 3.

The ratio of the power spectra in the *enhanced gravity* model and in  $\Lambda$ CDM is presented in Fig. 4. The accelerated growth of matter density perturbations translates into a significant scale-dependent enhancement of the power spectrum on scales that are below the Hubble radius today (i.e. with  $k \gtrsim 0.0003$  h/Mpc). The curve exhibits small wiggles due to a shift in the position of the peaks of baryon acoustic oscillations (cf. the shift of CMB peaks discussed in Sec. IV A). On sub-Hubble scales, the contribution of  $\delta\rho_\chi$  and  $\delta\rho_\xi$  to the total matter power spectrum is negligible<sup>19</sup>. Finally, let us point out that the curve in Fig. 4 must be taken with a grain of salt at  $k \gtrsim 0.1$  h/Mpc, where non-linearities become important.

*Shear model:* Our definition of the matter power spectrum refers to sub-Hubble wavelengths only, and also uses the assumption that  $\phi$  and  $\psi$  are equal in Eq. (37), which

<sup>17</sup> Strictly speaking, this definition makes sense only for modes well inside the horizon, where the Poisson equation is valid. However, this is sufficient for our study, because the power spectrum is actually measured for such modes only.

<sup>18</sup> We remind that in this work we consider the regime where  $c_\chi$ ,  $c_\Theta$  are of order one. If instead these velocities were very small, the fields  $\chi$  and  $\tilde{\xi}$  could in principle cluster also on scales much smaller than the Hubble radius.

<sup>19</sup> As mentioned above, this conclusion could change in a scenario where a tiny value of  $c_\chi$  or  $c_\Theta$  would be assumed.

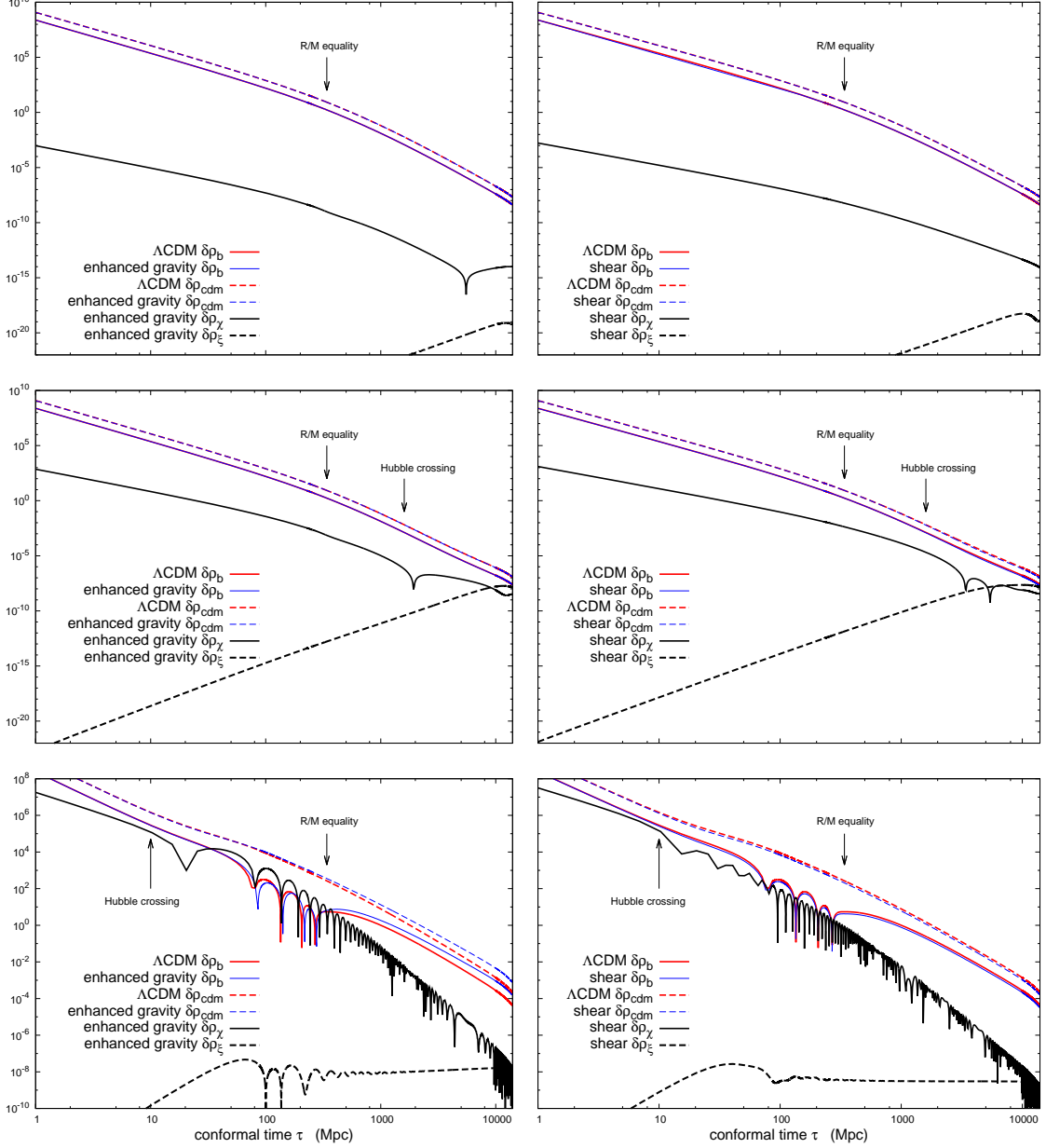


FIG. 3: Evolution of the transfer function of various energy density perturbations  $\delta\rho_i$  (arbitrary units) in the Newton gauge, for the *enhanced gravity* model (left) and the *shear* model (right), and for the three wavenumbers  $k = 10^{-7}\text{Mpc}^{-1}$  (top panels),  $k = 6 \times 10^{-4}\text{Mpc}^{-1}$  (middle panels) and  $k = 0.1\text{Mpc}^{-1}$  (bottom panels). For comparison, we show the evolution of  $\delta\rho_b$  and  $\delta\rho_{cdm}$  in the  $\Lambda\text{CDM}$  case. We also indicate the conformal time of Hubble crossing for the two largest wavenumbers, and the conformal time of radiation to matter equality.

leads to Eq. (45). Hence we need to check whether the anisotropic stress (responsible for a possible difference between the two metric perturbations, see Eq. (43)) vanishes inside the Hubble radius in the shear model. It is well-known that the anisotropic stress of neutrinos and of decoupled photons decays inside the Hubble radius, due to free-streaming. This conclusion also applies to the anisotropic stress of the khronon, due to the dynamics of the  $\chi$  field. For instance, during matter domination,

$\chi$  oscillates with an envelope decaying like  $\tau^{-3}$  on sub-Hubble scale, implying that its averaged energy density decays like  $\delta\rho_\chi \propto \tau^{-8} \propto a^{-4}$ . The contribution of the khronon anisotropic stress to the difference  $(\phi - \psi)$  is then oscillating with an envelope proportional to  $\tau^{-4} \propto a^{-2}$ . At the same time,  $\phi$  and  $\psi$  are almost constant. Hence the relative difference between  $\phi$  and  $\psi$  quickly becomes negligible, and our definition of the matter power spectrum on sub-Hubble scale is applicable.

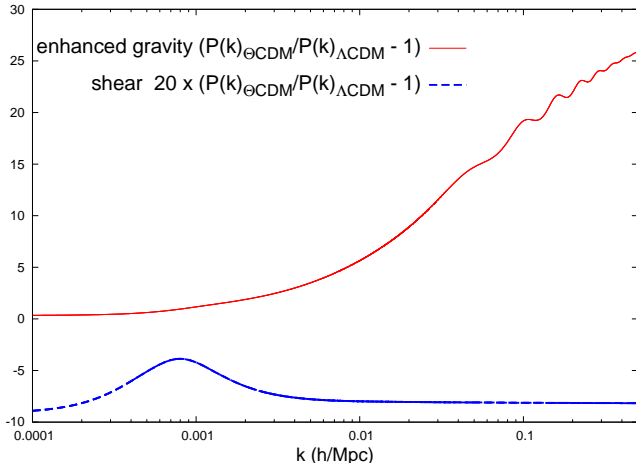


FIG. 4: Ratios of the matter power spectra in the two reference  $\Theta$ CDM models and in  $\Lambda$ CDM at redshift  $z = 0$ .

If we normalize perturbations to the same initial value of  $\psi$ , the evolution of  $(\delta\rho_{cdm}, \delta\rho_b)$  is identical above the Hubble scale in the  $\Lambda$ CDM and *shear* models. However, in the *shear* case, the anisotropic stress of the khronon cannot be neglected soon after the time of Hubble crossing. This leads to a smoothing of metric perturbations and to a suppression of  $\delta\rho_{cdm}$  and  $\delta\rho_b$  that is clearly visible in the lower right panel of Fig. 3. Well after Hubble crossing, the khronon anisotropic stress becomes negligible and  $(\delta\rho_{cdm}, \delta\rho_b)$  evolve like in  $\Lambda$ CDM, but with a constant offset coming from the suppression experienced soon after Hubble crossing.

This suppression is seen better in Fig. 4. For the chosen parameter values, the effect of the *shear* model is smaller than for the *enhanced gravity* model. In order to see clearly both effects with the same scale, we multiplied the difference between the power spectra in the *shear* model and in  $\Lambda$ CDM by 20. Inside the Hubble radius, the suppression of the power spectrum in the *shear* model is almost scale-independent. When approaching the current value of the Hubble scale, the suppression is reduced by the counteracting effect of additional density fluctuations in the  $\xi$  field. However, this reduction is only significant on scales that are too large to be observed with good precision (due to the sampling variance associated to a given survey). Besides, on such scales our definition of the matter power spectrum is no longer applicable<sup>20</sup>.

We reach the same conclusion as in the CMB case: on observable scales, the effect of pure *shear* models can be mimicked by an overall reduction of the primordial fluctuation amplitude, which suggests that these models are

<sup>20</sup> Like in the *enhanced gravity* model, we note that in a scenario with tiny values of  $c_\Theta$  or  $c_\chi$ , density fluctuations in the  $\xi$  or  $\chi$  field could in principle be significant on much smaller scales.

more weakly constrained than *enhanced gravity* models.

## V. COMPARISON WITH CURRENT DATA

We will now compare the khronometric  $\Theta$ CDM model to CMB and LSS data, using the parameter inference code MONTE PYTHON<sup>21</sup> [20]. For the CMB, we use here WMAP 7-year data [37], and SPT data from 2008 and 2009 [38]. Updating our analysis with recent Planck data [39] could give a small improvement on parameter constraints, without changing their order of magnitude. For LSS, we rely on galaxy power spectrum data from the WiggleZ redshift survey [40]. We choose to perform our runs in the synchronous gauge.

We include in the fit eight free cosmological parameters, which are the usual six free parameters of the minimal flat  $\Lambda$ CDM model, plus  $\beta$  and  $\beta + \lambda$  (this combination is chosen to facilitate the convergence of the chains). The parameter  $\alpha$  is fixed to  $2\beta$ , which is the condition for satisfying all bounds coming from Solar System tests in the khronometric model<sup>22</sup>. As far as cosmology is concerned, this condition is actually not necessary, but we implement it anyway in order to deal only with realistic models. We also vary three nuisance parameters describing the foreground contamination of SPT data, and we marginalize over these parameters following strictly the approach of Ref. [38].

We show our results for the Bayesian minimum credible interval of each parameter in Table II. The one-dimensional and two-dimensional posterior parameter distributions are displayed in Fig. 5 (omitting the three SPT nuisance parameters for clarity).

The  $\Theta$ CDM parameters are found to be weakly correlated with the six standard model parameters, and strongly correlated with each other. Isoprobability contours in the  $(\beta, \beta + \lambda)$  space have a complicated shape. They are very elongated along two directions of degeneracy, corresponding to  $\beta + \lambda \simeq 0$  and  $\beta \simeq 3/2(\beta + \lambda)$ . Away from these two special directions, the contours are more regular, and closer to an ellipse centered on the origin. The posterior probability peaks at  $(\beta, \beta + \lambda) \simeq (0, 0)$ , showing that the data brings no evidence in favor of the  $\Theta$ CDM model. The two directions of degeneracy can be interpreted as follows.

First, the case  $\beta + \lambda \simeq 0$  corresponds to  $\Sigma \simeq 0$  for our choice of  $\alpha$ . This is the region of pure *shear* models, discussed in the previous subsection. We already argued that the differences with  $\Lambda$ CDM are less important in this

<sup>21</sup> <http://montepython.net>

<sup>22</sup> We decided to focus only on the khronometric case, since from the comments after Eq. (42) it is clear that the bounds are stronger in this model than in the Einstein-aether case. This is confirmed by comparing our results with the constraints presented in Ref. [11].

$100 \omega_b$	$\omega_{cdm}$	$n_s$	$10^{+9} A_s$	$h$	$z_{reio}$	$\beta$	$\beta + \lambda$
$2.219^{+0.041}_{-0.044}$	$0.1205^{+0.0027}_{-0.0029}$	$0.9552^{+0.011}_{-0.011}$	$2.556^{+0.09}_{-0.092}$	$0.6782^{+0.013}_{-0.013}$	$10.05^{+1.2}_{-1.2}$	$< 0.05$	$< 0.012$

TABLE II: Mean values and 68% confidence limits of the minimum credible interval of the parameters of the khronometric  $\Theta$ CDM model. For  $\beta$  and  $\beta + \lambda$ , we show instead 95% upper limits.

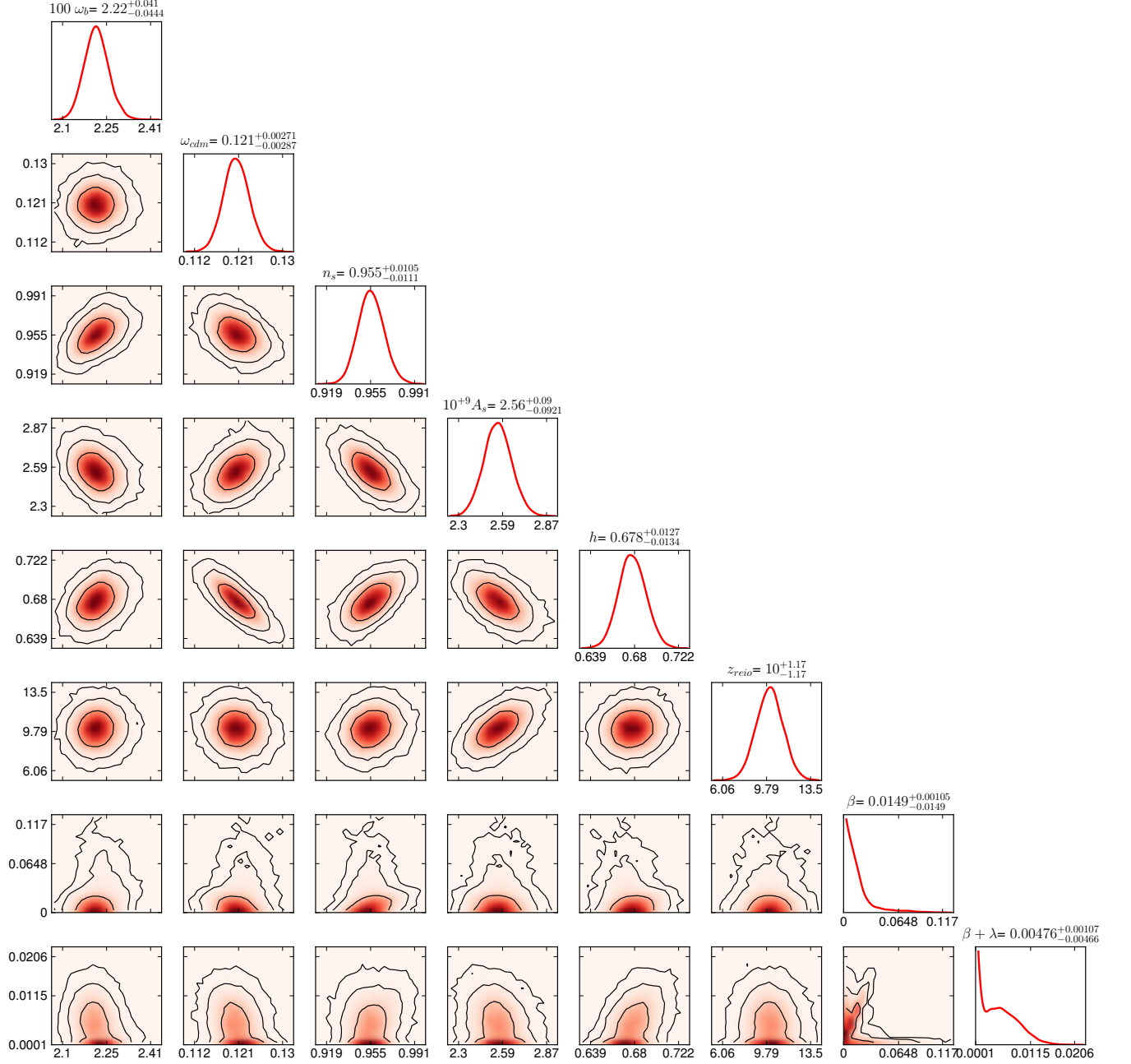


FIG. 5: Triangle plot showing the one-dimensional marginalized posterior distribution and the two-dimensional probability contours (at the 68, 95 and 99% confidence level) of the parameters of the khronometric  $\Theta$ CDM model.

case<sup>23</sup> than in the *enhanced gravity* case corresponding to the orthogonal direction  $\beta = 0$ . This explains the factor four difference between constraints on  $\beta$  and on  $\beta + \lambda$  in Table II.

The other case has a less straightforward interpretation. The relation  $\beta \simeq 3/2(\beta + \lambda)$  implies that the khronon has a squared sound speed  $c_\chi^2 \simeq 1/3$ , similar to that of neutrinos and of tightly coupled photons. Hence, for these models, the khronon does not introduce a new characteristic scale, and the oscillations seen in the lower left panel of Fig. 3 may mimic those of photons or neutrinos, thus lowering the sensitivity along this direction. We checked explicitly with the modified CLASS code that in this particular case, the sum of all effects described in the previous section (enhanced gravity, additional shear and extra clustering species) can be nearly cancelled at the level of CMB anisotropies by a variation of the standard cosmological parameters. This situation is analogous to the case of extra relativistic degrees of freedom, for which the impact of a small variation of  $N_{\text{eff}}$  on the CMB can be partially compensated by a variation of other parameters, leading to a well-known degeneracy between  $N_{\text{eff}}$  and  $H_0$  [41].  $\Theta$ CDM models with  $c_\chi^2 \simeq 1/3$  are not exactly equivalent to models with extra relativistic degrees of freedom, but their effect can be compensated in a similar way. This explains the weak correlation observed in Fig. 5 between standard parameters and  $\Theta$ CDM parameters. By comparing with a run based on CMB data only, we find that the inclusion of LSS data helps in breaking this degeneracy (by limiting enhanced gravity effects on the matter power spectrum), but even in presence of WiggleZ data, the degeneracy appears very clearly in Fig. 5.

## VI. CONCLUSIONS

In this work, we described the impact of the  $\Theta$ CDM model on cosmological observables, on scales where linear cosmological perturbation theory is valid. This model is an alternative to the  $\Lambda$ CDM scenario in which the acceleration of the universe expansion is caused by a dynamical scalar field  $\Theta$ . An important difference between this model and most quintessence models is that the action of the field  $\Theta$  is naturally protected from large ultraviolet corrections. In addition, the  $\Theta$ CDM model is embedded in a family of gravitation theories with broken Lorentz invariance, which may have an ultraviolet completion in

the framework of Hořava gravity. The latter theories are characterized by a time-like dynamical vector field  $u^\mu$  which defines a preferred time direction. Typical examples are the Einstein-aether and khronometric theories. The  $\Theta$ CDM model is the simplest extension of these theories to include a mechanism for cosmic acceleration. Under simple constraints on its parameters, it passes all local tests of gravity: Solar System dynamics, gravity wave emission, black hole structure. We have shown that the  $\Theta$ CDM model may produce observable effects on cosmological scales, constrained by current cosmological data, but still potentially detectable with future ones.

The background evolution in  $\Theta$ CDM is identical to  $\Lambda$ CDM. The only potential difference could come from a component playing the role of stiff matter, but in order to preserve primordial nucleosynthesis, we must assume that this component is too small for playing any role in late-time cosmology, and for affecting CMB and large scale structure observables. However, the evolution of cosmological perturbations is generically very different in the  $\Theta$ CDM and  $\Lambda$ CDM models. We studied the evolution equations of scalar perturbations in  $\Theta$ CDM and identified three different effects: *(i)* a renormalization of the matter contribution to the Poisson equation (i.e. a different self-gravity of matter perturbations), *(ii)* a new contribution to the anisotropic stress, and *(iii)* the presence of additional clustering degrees of freedom. The first two effects are generic for Lorentz violating gravitation theories based on a unit time-like vector, while the third one is specific to the dynamical realization of dark energy in  $\Theta$ CDM.

We implemented the equations of  $\Theta$ CDM in the Boltzmann code CLASS [19], in order to compute accurately the impact of the three effects *(i)*, *(ii)*, *(iii)*. We found that they affect the power spectrum of Cosmic Microwave Background anisotropies in a very particular way (shift in the position and amplitude of the peaks, and enhanced ISW), as can be seen in Fig. 2. Furthermore, they influence the shape of the matter power spectrum (different amplitude and slope on observable scales, shift in the position of baryon acoustic oscillations). These effects are shown in Figures 3 and 4.

To derive constraints on the free parameters of the khronometric  $\Theta$ CDM model (considering only parameter combinations satisfying Solar System tests), we used data from WMAP (7-year), from SPT (2008 and 2009 observations), and from the WiggleZ redshift survey. We ran the parameter inference code MONTE PYTHON [20] and found the bounds displayed in Table II and illustrated in Fig. 5. Quite remarkably, these bounds constrain deviations from general relativity to better than the percent level. They are stronger than those from several tests of gravitation, such as radiation damping of binary systems, or BBN. They are also stronger for the khronometric case studied in this paper than for the Einstein-aether model considered in Ref. [11], due to the absence of the effect *(i)* in the latter case. The vanishing of *(i)* in the Einstein-aether theory (once Solar System bounds are imposed)

<sup>23</sup> Under the condition  $\alpha = 2\beta$ , the velocity of the  $\chi$ -field is given by  $c_\chi^2 = \Sigma/(6\beta)$ . Thus, the limit  $\Sigma = 0$  formally corresponds to vanishing sound speed of the  $\chi$ -component. One could expect that this would lead to an amplification of the  $\chi$ -perturbations and, as a consequence, to strong constraints on the model. However, in practice,  $c_\chi$  never becomes smaller than  $\simeq 10^{-2}$  during the Monte Carlo sampling of the parameters and the clustering of  $\chi$  does not appear to be significant.

seems to be simply a coincidence.

The fact that our bounds are dominated by the effect (i) – modified self-gravity of the matter perturbations – suggests that they may have a wider application. The bound on the combination  $\beta + \lambda$  in Table II can be cast into the constraint on the discrepancy between the gravitational constants appearing in the Newton law and in the Friedmann equation,  $|G_N/G_{cos} - 1| < 0.018$  at 95% confidence level. Though in our model we cannot completely disentangle (i) from other effects, we believe that the above constraint will apply, at least by order of magnitude, to any theory predicting a time-independent discrepancy between  $G_N$  and  $G_{cos}$ . It represents an improvement compared to the bounds existing in the literature [42, 43].

Our analysis can be extended in several ways. First, we have only used the scalar sector of the theory. For the Einstein-aether case, the theory contains also propagating vector modes, whose influence on B-type CMB polarization could provide further observational tests [13, 15]. Second, the analysis can be updated with CMB data from Planck, and in the future, with large scale structure data from DES, LSST or Euclid. It would also be extremely interesting to go beyond the linear regime and try to understand the consequences of  $\Theta$ CDM for non-linear structure formation. Finally, to completely characterise possible deviations from Lorentz invariance in the context of cosmology, one can consider the option that this symmetry is violated also in the dark matter sector [27].

### Acknowledgements

We are grateful to Mikhail Ivanov, Gregory Gabadadze, Roman Scoccimarro and Takahiro Tanaka for useful discussions. D.B. and S.S. thank the organizers and participants of the Kavli IPMU Focus Week on Gravity and Lorentz Violations for the encouraging interest and valuable comments. S.S. thanks the Center for Cosmology and Particle Physics of NYU for hospitality during the completion of this work. This work was supported in part by the Grant of the President of Russian Federation NS-5590.2012.2 (S.S.), the Russian Ministry of Science and Education under the contract 8412 (S.S.), the RFBR grants 11-02-01528 (S.S.), 12-02-01203 (S.S.) and by the Dynasty Foundation (S.S.). J.L. and B.A. acknowledge support from the Swiss National Science Foundation.

### Appendix A: Initial conditions

The initial conditions for the system of differential equations describing the evolution of a given Fourier mode  $k$  are set in the radiation era, at a moment  $\tau_0$  when the wavelength associated to  $k$  is well outside the Hubble scale, i.e. when  $k \ll \mathcal{H}$ . As discussed in [4, 12], under broad assumptions, the dominant contribution to

the perturbations is provided by the growing adiabatic mode. In this Appendix we determine this mode analytically on super-Hubble scales using the equations of Sec. III B.

Taking into account that  $a \propto \tau$  during radiation domination ( $\tau$  stands for conformal time), and keeping only leading order terms in an expansion in  $(k/\mathcal{H}) \approx (k\tau)$ , we can simplify Eqs. (21a) and (21b):

$$\ddot{\chi} + \frac{2}{\tau}\dot{\chi} + \frac{2B}{\tau^2}\chi - \frac{G_0}{G_{cos}}\frac{H_\alpha}{\tau_\alpha}\tilde{\xi} + \frac{c_\chi^2}{2}\dot{h} + \frac{2\beta}{\alpha}\dot{\eta} = 0, \quad (\text{A1})$$

$$\ddot{\xi} + \frac{2}{\tau}\dot{\xi} = 0. \quad (\text{A2})$$

On the other hand, Eqs. (24), (28) can be rewritten as

$$\eta = \frac{G_0}{2k^2 G_{cos}}\frac{\dot{h}}{\tau} - \frac{3}{2k^2\tau^2}\frac{G_0}{G_{cos}}(R_\nu\delta_\nu + (1 - R_\nu)\delta_\gamma) - \frac{1}{2}\left[\alpha\dot{\chi} + \alpha(1 - B)\frac{\chi}{\tau}\right] - \frac{\alpha}{2k^2 c_\Theta^2}\frac{G_0}{G_{cos}}\frac{H_\alpha}{\tau_\alpha}\dot{\xi}, \quad (\text{A3})$$

$$\ddot{h} + \frac{\dot{h}}{\tau} + \frac{6}{\tau^2}(R_\nu\delta_\nu + (1 - R_\nu)\delta_\gamma) = -\frac{G_{cos}}{G_0}k^2\alpha(1 + B)\left(\dot{\chi} + \frac{\chi}{\tau}\right) - \frac{\alpha H_\alpha \dot{\xi}}{c_\Theta^2 \tau_\alpha}, \quad (\text{A4})$$

where  $R_\nu$  is the ratio of the density of neutrinos to the total radiation density. Since we have not modified the matter sector of the theory, the solutions for matter perturbations in the super-Hubble regime coincide with Eqs. (92) of [31]. Note that we have left aside the remaining pair of Einstein equations (26), (30), that are redundant and automatically satisfied by the solution (A7)–(A10).

At initial time  $\tau_0$ , the  $\Theta$ -field contribution to the total energy density is negligible. It is natural to expect that its fluctuations can also be neglected, which corresponds to dropping off the terms containing  $\xi$  in Eqs. (A1), (A3) and (A4). Let us find the precise conditions under which this is possible. The non-decaying solution of (A2) is

$$\tilde{\xi} = \tilde{\xi}_0, \quad (\text{A5})$$

where  $\tilde{\xi}_0$  is a constant implying that the  $\tilde{\xi}$  contribution drops out of Eqs. (A3), (A4). As for Eq. (A1), we find that the  $\tilde{\xi}$ -term is negligible provided the following condition is satisfied:

$$\tilde{\xi}_0 \ll \frac{\tau_\alpha \tau_0}{H_\alpha} h_0, \quad (\text{A6})$$

where we have used the expression (A7a) for  $h$  and have assumed  $c_\Theta, c_\chi \sim 1$ . This inequality is the condition for having negligible isocurvature perturbations in the  $\tilde{\xi}$ -field. It is likely to be satisfied under plausible assumptions about the origin of the primordial  $\xi$ -perturbations [4]. However, this statement must be taken with a grain of salt: a detailed theory of the  $\Theta$ -field dynamics starting from the inflationary epoch is required to put it on the

solid ground. We leave developing such a theory for the future. In the present work we will set  $\tilde{\xi}_0$  to zero in the numerical simulations.

For other fields we use the ansatz<sup>24</sup> (cf. [31]):

$$h = h_0\tau^2 + h_1\tau^4, \quad \eta = \eta_0 + \eta_1\tau^2, \quad (\text{A7a})$$

$$\delta_\gamma = \delta_{\gamma 0}\tau^2 + \delta_{\gamma 1}\tau^4, \quad \delta_\nu = \delta_{\nu 0}\tau^2 + \delta_{\nu 1}\tau^4, \quad (\text{A7b})$$

$$\theta_\gamma = \theta_{\gamma 0}\tau^3, \quad \theta_\nu = \theta_{\nu 0}\tau^3, \quad (\text{A7c})$$

$$\sigma_\nu = \sigma_{\nu 0}\tau^2, \quad \chi = \chi_0\tau^3. \quad (\text{A7d})$$

From the matter equations (Eqs. (92) of [31]) we obtain the standard relations:

$$\delta_{\gamma 0} = -\frac{2}{3}h_0, \quad \delta_{\gamma 1} = \frac{k^2}{54}h_0 - \frac{2}{3}h_1, \quad (\text{A8a})$$

$$\delta_{\nu 0} = -\frac{2}{3}h_0, \quad \delta_{\nu 1} = \frac{k^2}{30}h_0 + \frac{4k^2}{45}\eta_1 - \frac{2}{3}h_1, \quad (\text{A8b})$$

$$\theta_{\gamma 0} = -\frac{k^2}{18}h_0, \quad \theta_{\nu 0} = -\frac{k^2}{10}h_0 - \frac{4k^2}{15}\eta_1, \quad (\text{A8c})$$

$$\sigma_{\nu 0} = \frac{2}{15}h_0 + \frac{4}{5}\eta_1. \quad (\text{A8d})$$

To find the relations between the fields  $h_0, h_1, \eta_1$  we use (A3), (A4) and (A1). In the leading order the first equations is satisfied identically, while the second yields

$$\eta_0 = \frac{2G_0}{k^2 G_{\text{cos}}} h_0. \quad (\text{A9})$$

Considering the subleading order in (A3), (A4) and the leading order in (A1) we obtain

$$\chi_0 = -\frac{c_\chi^2}{2(6+B)}h_0 - \frac{2\beta}{\alpha(6+B)}\eta_1, \quad (\text{A10a})$$

$$h_1 = \left[ -\frac{k^2(5+4R_\nu)}{540} + \frac{\alpha k^2 c_\chi^2(1+B)}{6(6+B)} \frac{G_{\text{cos}}}{G_0} \right] h_0 - \left[ \frac{2k^2 R_\nu}{45} - \frac{2k^2 \beta(1+B)}{3(6+B)} \frac{G_{\text{cos}}}{G_0} \right] \eta_1, \quad (\text{A10b})$$

$$\eta_1 = -\frac{h_0}{6} \frac{5+4R_\nu - \frac{45}{2}\alpha c_\chi^2 \frac{G_{\text{cos}}}{G_0}}{15 \frac{G_{\text{cos}}}{G_0} (1-\beta) + 4R_\nu}. \quad (\text{A10c})$$

It is now straightforward to check that the obtained solution satisfies the remaining Einstein's equation (26), (30).

To summarize, the adiabatic mode is given by Eqs. (A7) with the coefficients related by (A8), (A9), (A10) to the single constant  $h_0$  setting the overall normalization. To these expressions we add the standard adiabatic initial conditions for baryons and dark matter [31]:

$$\delta_{\text{cdm}} = \delta_b = \frac{3}{4}\delta_\gamma, \quad \theta_{\text{cdm}} = 0, \quad \theta_b = \theta_\gamma. \quad (\text{A11})$$

We cross-checked the validity of our initial conditions using the numerical code. When fixing initial conditions at  $\tau_0$ , we find that over an extended range of time above  $\tau_0$ , the numerical solutions for  $(h, \eta, \chi)$  and for all density perturbations remain equal to their analytic expressions in Eqs. (A7)-(A10). Hence, the above initial conditions correctly describe the attractor solution of the full system of equations that is compatible with the adiabatic condition (A11) for matter fields. At leading order, the attractor solution for the field  $\tilde{\xi}$  is given by

$$\tilde{\xi} = \frac{(c_\Theta k\tau)^2}{42H_\alpha \tau_\alpha} \chi \quad (\text{A12})$$

and evolves proportionally to  $\tau^6$ . Since this solution is too small to back-react on other fields, it makes no difference to fix the initial  $\tilde{\xi}$  to the above solution or to zero (in the latter case,  $\tilde{\xi}$  reaches very quickly the attractor solution).

When deriving initial conditions, we assumed full radiation domination, and neglected all corrections related to the contribution of non-relativistic matter to the expansion rate. Hence our initial conditions are accurate only if imposed at very early time. We decreased  $\tau_0$  in the code until getting very stable results. This is the case for the value  $\tau_0 = 10^{-2}$ Mpc, that we adopted in all simulations.

- 
- [1] L. Amendola and S. Tsujikawa, "Dark energy. Theory and Observations", Cambridge University Press (2010), 506 p.
- [2] L. Amendola *et al.* [Euclid Theory Working Group Collaboration], arXiv:1206.1225 [astro-ph.CO].
- [3] E. J. Copeland, M. Sami and S. Tsujikawa, Int. J. Mod. Phys. D **15** (2006) 1753 [hep-th/0603057].
- [4] D. Blas and S. Sibiryakov, JCAP **1107** (2011) 026 [arXiv:1104.3579 [hep-th]].
- [5] T. Jacobson and D. Mattingly, Phys. Rev. D **64**, 024028 (2001) [arXiv:gr-qc/0007031].
- [6] T. Jacobson, PoS **QG-PH**, 020 (2007) [arXiv:0801.1547 [gr-qc]].
- [7] P. Horava, Phys. Rev. D **79**, 084008 (2009) [arXiv:0901.3775 [hep-th]].
- [8] D. Blas, O. Pujolas and S. Sibiryakov, Phys. Rev. Lett. **104** (2010) 181302 [arXiv:0909.3525 [hep-th]].
- [9] D. Blas, O. Pujolas, S. Sibiryakov, JHEP **1104**, 018 (2011) [arXiv:1007.3503 [hep-th]].
- [10] T. Jacobson, Phys. Rev. D **81**, 101502 (2010) [Erratum-ibid. D **82**, 129901 (2010)] [arXiv:1001.4823 [hep-th]].
- [11] J. A. Zuntz, P. G. Ferreira and T. G. Zlosnik, Phys. Rev. Lett. **101** (2008) 261102 [arXiv:0808.1824 [gr-qc]].
- [12] T. Kobayashi, Y. Urakawa and M. Yamaguchi, JCAP



- 1004**, 025 (2010) [arXiv:1002.3101 [hep-th]].
- [13] C. Armendariz-Picon, N. F. Sierra and J. Garriga, JCAP **1007** (2010) 010 [arXiv:1003.1283 [astro-ph.CO]].
- [14] S. M. Carroll and E. A. Lim, Phys. Rev. D **70**, 123525 (2004) [arXiv:hep-th/0407149].
- [15] M. Nakashima and T. Kobayashi, Phys. Rev. D **84** (2011) 084051 [arXiv:1103.2197 [astro-ph.CO]].
- [16] B. Li, D. Fonseca Mota and J. D. Barrow, Phys. Rev. D **77** (2008) 024032 [arXiv:0709.4581 [astro-ph]].
- [17] T. G. Zlosnik, P. G. Ferreira and G. D. Starkman, Phys. Rev. D **77** (2008) 084010 [arXiv:0711.0520 [astro-ph]].
- [18] W. Donnelly and T. Jacobson, Phys. Rev. D **82** (2010) 064032 [arXiv:1007.2594 [gr-qc]].
- [19] D. Blas, J. Lesgourgues and T. Tram, JCAP **1107** (2011) 034 [arXiv:1104.2933 [astro-ph.CO]].
- [20] B. Audren, J. Lesgourgues, K. Benabed and S. Prunet, arXiv:1210.7183 [astro-ph.CO].
- [21] V. A. Kostelecky and N. Russell, Rev. Mod. Phys. **83** (2011) 11 [arXiv:0801.0287 [hep-ph]].
- [22] B. Z. Foster, Phys. Rev. D **72**, 044017 (2005) [gr-qc/0502066].
- [23] O. Pujolas and S. Sibiryakov, JHEP **1201**, 062 (2012) [arXiv:1109.4495 [hep-th]].
- [24] S. Groot Nibbelink and M. Pospelov, Phys. Rev. Lett. **94**, 081601 (2005) [hep-ph/0404271].
- [25] G. Bednik, O. Pujolas and S. Sibiryakov, *to appear*.
- [26] E. Barausse, T. Jacobson and T. P. Sotiriou, Phys. Rev. D **83** (2011) 124043 [arXiv:1104.2889 [gr-qc]].
- [27] D. Blas, M. M. Ivanov and S. Sibiryakov, JCAP **1210** (2012) 057 [arXiv:1209.0464 [astro-ph.CO]].
- [28] B. Z. Foster, Phys. Rev. D **73** (2006) 104012 [Erratum-ibid. D **75** (2007) 129904] [gr-qc/0602004].
- [29] D. Blas and H. Sanctuary, Phys. Rev. D **84** (2011) 064004 [arXiv:1105.5149 [gr-qc]].
- [30] E. A. Lim, Phys. Rev. D **71** (2005) 063504 [astro-ph/0407437].
- [31] C. P. Ma and E. Bertschinger, Astrophys. J. **455** (1995) 7 [arXiv:astro-ph/9506072].
- [32] S. Dutta and R. J. Scherrer, Phys. Rev. D **82** (2010) 083501 [arXiv:1006.4166 [astro-ph.CO]].
- [33] D. Mattingly, Living Rev. Rel. **8**, 5 (2005) [gr-qc/0502097].
- [34] A. Lue, R. Scoccimarro and G. Starkman, Phys. Rev. D **69** (2004) 044005 [astro-ph/0307034].
- [35] G. D’Amico, G. Gabadadze, L. Hui and D. Pirtskhalava, arXiv:1206.4253 [hep-th].
- [36] F. Bernardeau, S. Colombi, E. Gaztanaga and R. Scoccimarro, Phys. Rept. **367**, 1 (2002) [astro-ph/0112551].
- [37] E. Komatsu *et al.* [WMAP Collaboration], Astrophys. J. Suppl. **192** (2011) 18 [arXiv:1001.4538 [astro-ph.CO]].
- [38] R. Keisler, C. L. Reichardt, K. A. Aird, B. A. Benson, L. E. Bleem, J. E. Carlstrom, C. L. Chang and H. M. Cho *et al.*, Astrophys. J. **743** (2011) 28 [arXiv:1105.3182 [astro-ph.CO]].
- [39] P. A. R. Ade *et al.* [Planck Collaboration], arXiv:1303.5062 [astro-ph.CO].
- [40] D. Parkinson, S. Riemer-Sorensen, C. Blake, G. B. Poole, T. M. Davis, S. Brough, M. Colless and C. Contreras *et al.*, arXiv:1210.2130 [astro-ph.CO].
- [41] J. Lesgourgues, G. Mangano, G. Miele and S. Pastor, “Neutrino cosmology”, Cambridge University Press (2013)
- [42] G. Robbers, N. Afshordi and M. Doran, Phys. Rev. Lett. **100**, 111101 (2008) [arXiv:0708.3235 [astro-ph]].
- [43] R. Bean and M. Tangmatitham, Phys. Rev. D **81** (2010) 083534 [arXiv:1002.4197 [astro-ph.CO]].